crystals

MDPI

Article

Investigation of Hardness and Microanalysis of Sintered Aluminum-Based Supplemented Metal Matrix Machined Composites

Muhammad Raheel Bhutta [1,†], Fouzia Gillani [2,†], Taiba Zahid [3], Saira Bibi [4,*] and Usman Ghafoor [5,6,*]

[1] Department of Electrical and Computer Engineering, University of UTAH Asia Campus, Incheon 21985, Republic of Korea; raheel.bhutta@utah.edu
[2] Department of Mechanical Engineering & Technology, Government College University, Faisalabad 37000, Pakistan; fouziagillani@gcuf.edu.pk
[3] NUST Business School, National University of Sciences and Technology (NUST), Islamabad 44000, Pakistan; drtaiba@nbs.nust.edu.pk
[4] Department of Materials Science and Engineering, Pak-Austria Fachhochschule Institute of Applied Sciences and Technology, Haripur 22620, Pakistan
[5] School of Mechanical Engineering, Pusan National University, Busan 46241, Republic of Korea
[6] Department of Mechanical Engineering, Institute of Space Technology, Islamabad 44000, Pakistan
* Correspondence: saira.bibi@fcm3.paf-iast.edu.pk (S.B.); usman@pusan.ac.kr (U.G.)
† These authors contributed equally to this work.

Abstract: Aluminum metal matrix composites (AMMCs) have become increasingly ubiquitous in the fields of aerospace and automobile businesses due to their lightweight properties. Their machining is a challenging task because of the presence of supplemented particles, also called reinforcements. As the wt% of the supplemented particles changes, the morphological and machining behaviors of the AMMCs change. The present work is focused on exploring the thermo-mechanical properties of AMMCs which would help in AMMC applications in the aerospace industry with a new collection of composites containing silicon carbide (SiC) and zircon/zirconium silicate ($ZrSiO_4$) as supplements in wt% of 5%, 20%, 30%, and 40%. Uniform binary and hybrid sample pallets are prepared by powder metallurgy (PM). The said samples are sintered and then machined using wire electric discharge machining (WEDM) employing brass wire with a feed rate of 2 to 3 mm/min. Also, analysis of porosity and recast layer formation is performed via the microstructure, scanning electron microscopy (SEM), and energy dispersive spectroscopy (EDS). Some interesting and useful findings are obtained which can extend the applications of AMMCs in automobiles and the aerospace industry. The results reveal that temperature and wt% are playing their significant roles in the changes in the thermo-mechanical properties of AMMCs. Mathematical equations via regression analysis using Minitab 17 and Excel are developed for the congruence of experimental data. Analysis of Variance (ANOVA) is also performed. Hence, the most optimized relationships for the best machining output are established and presented in this proposed study.

Keywords: aluminum metal matrix composites; analysis of variance; electric discharge machining; regression analysis; scanning electron microscopy

Citation: Bhutta, M.R.; Gillani, F.; Zahid, T.; Bibi, S.; Ghafoor, U. Investigation of Hardness and Microanalysis of Sintered Aluminum-Based Supplemented Metal Matrix Machined Composites. *Crystals* **2023**, *13*, 1347. https://doi.org/10.3390/cryst13091347

Academic Editors: Yue Li, Dengshan Zhou and Hailiang Yu

Received: 28 July 2023
Revised: 21 August 2023
Accepted: 22 August 2023
Published: 4 September 2023

1. Introduction

Aluminum has a significant and pervasive use in both industrial and consumer applications due to its advantageous properties as a lightweight, nonmagnetic, malleable, and ductile element [1]. In recent applications, aluminum is used in combination metals, ceramics, or organic components by making them as aluminum metal matrix composites (AMMCs) to improve the physical and mechanical properties of the base metal, like hardness, quality, resistance to wear, conductivity, stiffness, etc., in order to trigger attention towards their most advanced applications in the aerospace and automobile industries [2].

Composite materials reinforced with materials imparting good mechanical properties have taken a wider place in industry for their high material efficiencies. The methods of preparation for such composites are also very important, as they contribute towards the thermo-mechanical properties of the composites [3,4]. The reinforcements must be non-reactive and stable enough at working temperatures and also possess superior mechanical properties [5]. Among many supplemented materials like carbides and nitrides, silicon carbide (SiC) has an added advantage over others due to its low density, better heat conductivity, and high elastic modulus, along with its easy availability. It is also inexpensive when compared to the others [6]. AMMCs with varying wt% of SiC also revealed that hardness and tensile strength increases, along with the reduction in percentage elongation, when increasing the wt% of SiC up to 25% [7]. It was also observed that AMMCs with 10% SiC were more favorable for applications in industries like aerospace, automobile, and military parts due to their supercilious mechanical properties. Few properties are directly affected by the addition of supplementary materials, like hardness, roughness, and wear, especially [4,5].

Hardness, tensile strengths, and impact strengths of AMMCs supplemented with SiC increase when increasing the wt% of reinforcement [8–10]. In the preparations of AMMCs with SiC as supplements, micro hardness, clustered regions, and porosities increase as the wt% of supplements increase along with the reduction in the particle size of the reinforcement [11]. As far as their machining is concerned, non-traditional or advanced mechanisms are required for the accurate machining of AMMCs, e.g., laser beam machining (LBM) and water jet machining (WJM). But these machining methods are limited to linear machining only [3].

Despite other non-traditional machining methods, the electrical discharge machining (EDM) process was found to be the most promising one for the removal of material from AMMCs. EDM removes the material by erosion through melting and vaporizing in the presence of dielectric fluid [12–14]. Spark erosion occurs between the tool and the workpiece gap [15]. The machinability of MMCs is dependent upon the processes of machining being adopted, along with the proper selection of the process material and operating parameters, irrespective of the natures of the AMMCs [16]. Furthermore, formation of a recast layer during machining must be removed without distorting the surface integrity, as it imparts tensile residual stresses, resulting in cracking and low fatigue strength in the material being machined [17].

Machining explorations of properties, such as elemental analysis, micro hardness, porosity, surface roughness, etc., can be performed by using X-Ray diffraction (XRD), scanning electron microscopy (SEM), electron probe microscopic analysis (EPMA), and differential thermal analysis (DTA). The characterization results offer important, new information about the composite powder's microstructure and phase distribution [18]. The uniform distribution of supplemented particles results in greater strength and imparts high hardness, which eventually leads to high resistance to wear [19,20]. Moreover, in EDM, brass electrode wire is found to be more reliable when compared to others because of its higher material removal rate (MRR); non-electric parameters of EDM, like flushing pressure, also contribute towards MRR.

Therefore, it is concluded that the machining and modeling of machined profiles of AMMCs are yet to be explored in many aspects [21]. Hybrid aluminum metal matrix composites (HAMMCs) are the foremost engineering materials due to their outstanding characteristics and applications. The machining of HAMMCs paved a new path to explore machining behaviors and their effects on the applications of these modern materials in the industry [22,23]. It was also found that the cutting processes of AMMCs are not completely explored [24]. The machining of AMMCs is quite difficult due to the presence of hard supplementary particles. They have higher levels of hardness compared to tools made up of carbide and high-speed steel (HSS) [25]. Out of advanced non-conventional machining processes, EDM is found to be the more reliable thermal process, in which the material is removed precisely by small spark erosion [26]. However, the EDM is established enough in

many sophisticated industries like aerospace, automotive, and surgical instruments [27]. The machining behaviors of SiC-supplemented AMMCs have not been completely explored until now in the literature. Therefore, in the current study, aluminum is selected as a matrix material supplemented by SiC and $ZrSiO_4$ particles to produce composites by the PM route. Varying wt% of SiC and $ZrSiO_4$ are added and then machined. The machine profile is investigated for microstructure investigation along with hardness of the machined surface.

2. Methodology

2.1. Sample Preparation

The pure aluminum powder is used for the preparation of MMCs. The average particle size (APS) range was 43–45 µm. Silicon carbide micro particles (SiC) with APS were 37–45 µm. The APS of zircon was <50 nm. Particle type and discontinuous reinforcements were used. All powders were 99% pure. The hardness of AMMCs was be increased with the increase in wt% of $ZrSiO_4$ and SiC-reinforced MMCs [28]. The challenging task lay in the preparation of the samples due to low wettability of the supplementary material phase. Therefore, the preparation of AMMCs could not be possible by traditional casting methods [29]. A few properties of SiC powder and $ZrSiO_4$ are mentioned in Table 1.

Table 1. Property table for reinforcements [25].

Elastic Modulus	SiC	$ZrSiO_4$
Elastic Modulus	410 GPa	275 GPa
Thermal Conductivity	30–40 W/mK	3.5 W/Mk (at 600 k)

The first step of preparation of samples was to weigh the powder as required. For this purpose, powders were weighted using a digital weight balance of least 0.1 mg. The measured weights of powders were ball-milled for one hour with the help of 35 balls of steel (molybdenum each of size 5 mm) to further grind the mixture. A 10:1 ball-to-powder ratio (BPR) was used during the mixing of powders in order to achieve homogeneous mixing. Powders were mixed at 150 rpm for 60 min, respectively. After mixing, powders were fed into the uniaxial hydraulic press with the help of a die as shown in Figure 1 with a diameter of 20 mm, generating a pallet of the sample as shown on the left side of Figure 2.

Figure 1. Die assembly used for making compact samples with the help of hydraulic press. The diameter of samples to be prepared is 20 mm and the thickness is 4 mm.

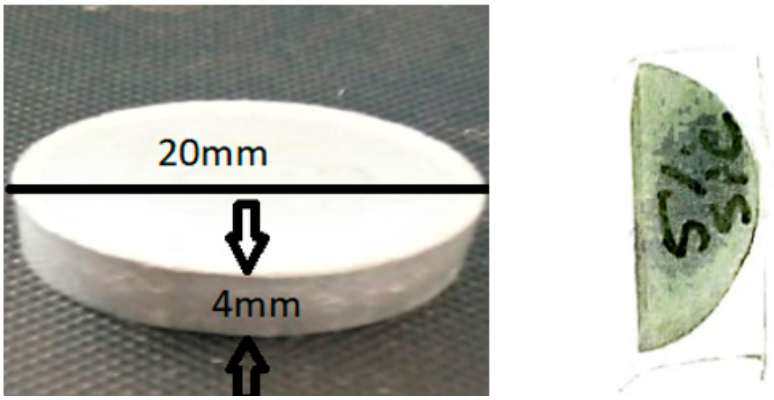

Figure 2. The left side of the figure shows fabricated AMMC while the right side shows a machined sample.

The mixture was compacted with the help of a hydraulic press for 2 min under a pressure of 196 Mpa. After 2 min, the press was released and the sample was removed from the circular die.

After compaction of binary and hybrid AMMCs, the samples were fed to sintering furnace to heat them at different temperatures ranging from 500 °C to 1100 °C. Sintered samples, as shown on the left side of Figure 1, were subjected to machining, and then the porosity, chemical composition, and mechanical properties were examined, as well as the hardness of the machined surface. The hardness of the machined samples was measured with the Vickers hardness tester. The hardness was measured from the size of an impression generated under load by a pyramid-shaped diamond indenter. Here, the load of 980.7 mN was taken for 10 s. Furthermore, the SEM analysis was conducted to study the microstructure examination using FESEM [30] as shown in Figure 3.

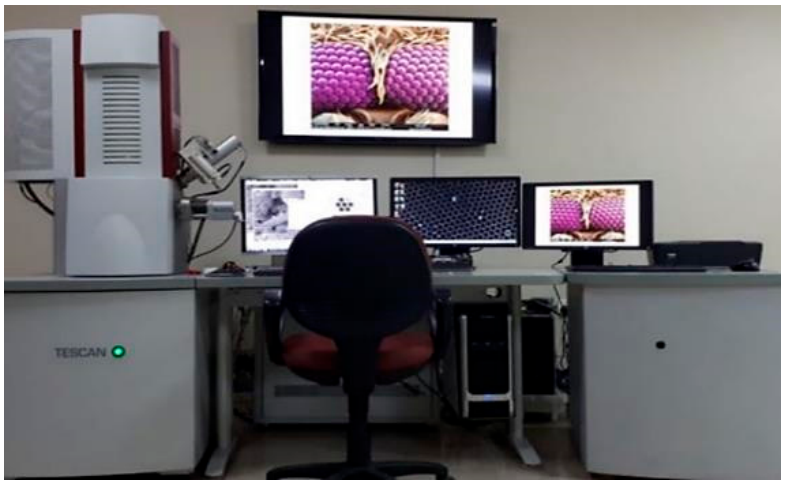

Figure 3. Field emission scanning electron microscope (FESEM) used for EDS analysis and microstructure images.

For the validation of experimental results, mathematical equations were estimated for each input parameter using regression analysis. Fabricated sample (20 mm diameter and 4 mm thickness) compositions and sintering conditions are mentioned in the published work of part of this research before machining [9]. The plan of the experiment mentioning the designed ratio of reinforcements along with the selected sintering temperature and sintering time in sintering furnace is shown in Table S1 of the attached Supplementary File.

2.2. Machining of Samples

Machining of AMMCs is a challenging task because of the abrasive nature of supplemented particles. Traditional machining processes such as turning, milling, or drilling are adopted for machining MMCs. But low surface integrity and accuracy of the machined samples hindered the adoption of conventional machining for MMCs [31].

In the current study, the WEDM with a brass wire 0.25 mm in diameter was used, keeping the pulse on/off time at constant values during the operation. The wire feed rate was 2 to 3 mm/min. WEDM is a non-conventional thermal machining process in which a wire made up of copper, brass or molybdenum can be used as an electrode [32]. It is pertinent to know that the conductivity of the electrode and work-piece is mandatory for the material removal as series of successive sparks are the source for cutting [33–35]. Electric sparks produce heat at a temperature of 8000–12,000 °C, causing melting and vaporization of the work-piece in the local surface layers. During the WEDM process, dielectric fluid is consistently flushed in and out to carry the eroded material away [36]. The surface of the work-piece is cooled side by side and solidified at a very high rate due to the high thermal conductivity of water. This solidification of the top surface of the work-piece results in the formation of a recast layer [37]. There are certain electrical and nonelectrical parameters of WEDM which are needed to be selected at appropriate levels before the start of machining [38]. Table 2 shows the machining conditions of WEDM. The samples are cut in a transverse direction across the diameter.

Table 2. Machining conditions of WEDM.

Machining Conditions	Symbol	Unit	Values
Gap voltage	V_p	mV	50
Pulse-on time	T_{ON}	µs	12
Pulse-off-time	T_{OFF}	µs	14
Wire feed rate	WFS	mm/min	2–3
Wire diameter	WD	Mm	0.25

3. Results and Discussions

Estimation of elements in AMMC reinforced with SiC and $ZrSiO_4$ with varying wt% was performed by EDS analysis using SEM. The images obtained showed that porosity, high pressure and close compaction of powder generates dense microstructure which improves the heat conduction capacity and strength of AMMCs. The irregular and random shapes of particles in the composite were observed. It was also observed that as the wt% of the supplements increases, consolidation of samples from solid state to liquid state occurs in the case of all twelve samples. Moreover, the recast layer was assumed to increase the surface hardness of machined samples.

3.1. EDS Analysis of Samples

Optical microscopic examination of the composite reveals the presence of reinforcement particles in the form of clusters as shown in Figure 4 of hybrid AMMCs. Machining of such samples is not obvious as well.

EDS analysis of the samples containing 40% by weight of SiC confirms that SiC particles are present in the synthesized composites as shown in Figure 5, whereas Table 3 presents the wt% of each constituent element.

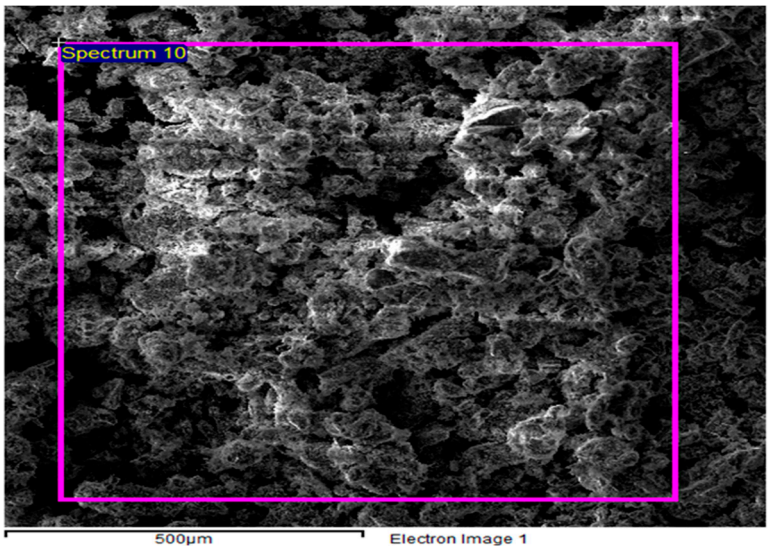

Figure 4. Clustering zone observed in hybrid AMMCs.

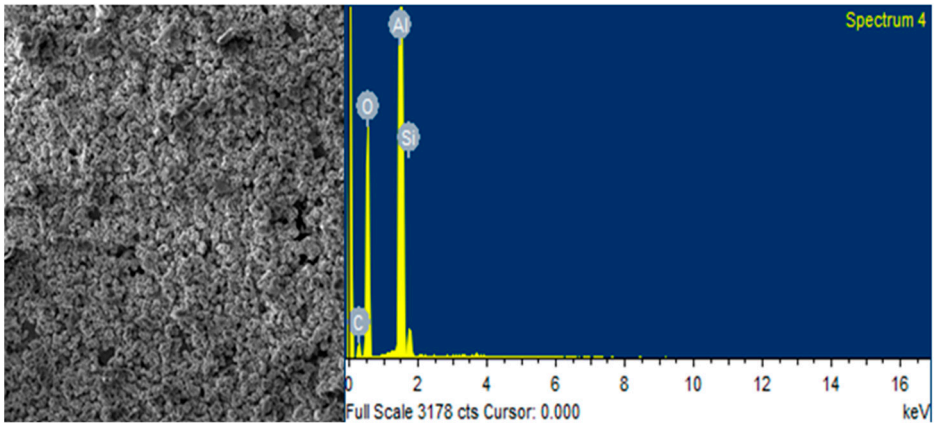

Figure 5. EDS analysis of AMMC with 40% SiC as a supplement. Left side shows microstructure image and right side presents the graphical presentations of elements included in composite showing their wt%.

Table 3. List of elements found as a result of EDS using SEM in the Al + 40% SiC supplemented composites.

Elements	Weight%	Atomic%
Al	44.98	32.44
Si	1.71	1.18
C	3.77	6.11
O	49.54	60.26

It is important to note that oxides were also formed during the machining of AMMCs. Similarly, the case of hybrid composite with SiC and $ZrSiO_4$ is shown in Figure 6 and wt% is presented in Table 4.

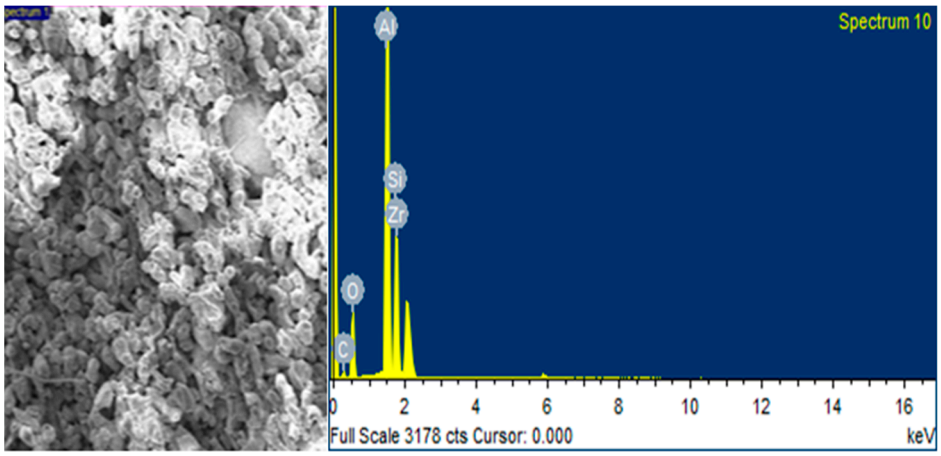

Figure 6. EDS analysis of AMMC with 20% SiC and 30% $ZrSiO_4$ as a supplement. Left side shows microstructure image and right side presents the graphical presentations of elements included in composite showing their wt%.

Table 4. List of elements found as a result of EDS using SEM in the Al + 30% SiC + 20% $ZrSiO_4$ supplemented composites.

Elements	Weight%	Atomic%
Al	44.55	37.34
Si	13.59	10.95
C	10.83	20.39
O	20.28	28.66
Zr	10.75	2.67

3.2. Porosity

Agglomerations or clustering of the reinforcements of varying size and shape are observed in Figure 7; they result in particulate-rich and particulate-depleted regions.

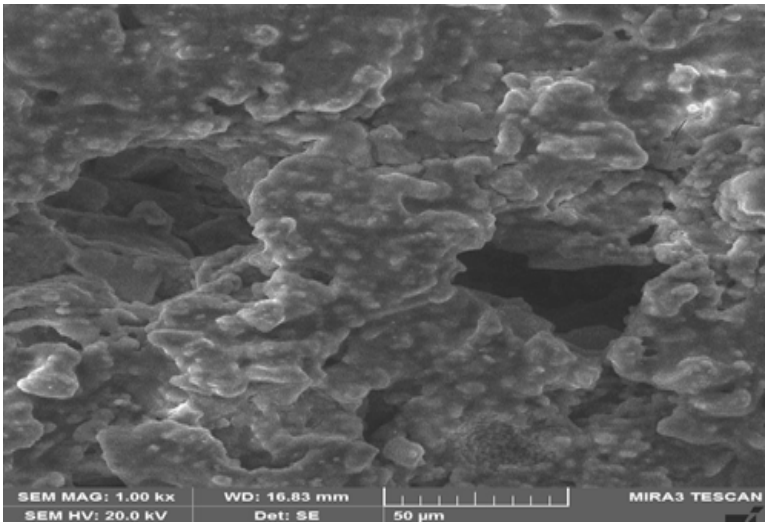

Figure 7. Porosity is shown in machined AMMC with 40% SiC.

Porosity and depleted zones were seen in the images obtained via SEM because of the difference between the melting points of base metal and supplementary materials (composition); however, one profound aspect which can be a next-level investigation is the compaction pressure selected in this research since compaction pressure is inversely proportional to porosity. It is also observed in the previous studies that a small increase in

wt% of reinforcements causes drastic porosity due to the clustering and agglomeration at high concentrations of supplements [39]. Hence, it can be concluded that supplementary particles act as a barrier between rearrangement and diffusion of reinforcements resulting in higher porosity, irrespective of the sintering temperature.

3.3. Hardness of Machined Samples

The hardness of machined samples may be enormously affected due to the heating and machining of samples. For this reason, investigation of hardness was performed with the Vicker hardness tester. Hardness of the samples was tested by a micro indenter with a diamond probe using a force of 980.7 mN for 10 s with a high-voltage harness tester at room temperature. It was observed that the Al-SiC binary composite matrix contains a wt% of 5 and 20, whereas the hybrid composite of Al-SiC 5%–$ZrSiO_4$ 40% has approximately the same hardness. It is important to note that the SiC wt% was at its lowest value in the above cases. As the wt% of SiC increases, the hardness of AMMCs increases. Meanwhile, the smallest value of hardness, i.e., 13.83 HV, was observed for the composite with 40% of $ZrSiO_4$. The observed trend in this study shows that as the wt% of $ZrSiO_4$ increases, the hardness decreases. However, the maximum hardness out of all twelve samples is observed, i.e., 104.06 HV, for AMMC with 20 wt% of $ZrSiO_4$. It is important to note that as the sintering temperature increases, the hardness of the machined samples increases. However, in the case of AMMCs supplemented with $ZrSiO_4$, hardness decreases with the increase in temperature beyond 700 °C. Sintering time does not impart much to the change in hardness of machined samples. Table 5 shows the values measured for hardness along with the standard deviation against each measurement.

Table 5. Hardness values for machined samples.

Sample	Type	Sample	Mean Hardness (HV) ± STD
Al-SiC	Binary	S1	30.8 ± 2.4
		S2	36.0 ± 2.2
		S3	59.4 ± 2.4
		S4	67.7 ± 3.1
Al-$ZrSiO_4$	Binary	S5	25.4 ± 2.2
		S6	104.0 ± 2.4
		S7	60.2 ± 3.1
		S8	13.8 ± 1.8
Al-SiC-$ZrSiO_4$	Hybrid	S9	29.8 ± 2.2
		S10	49.4 ± 2.6
		S11	50.6 ± 2.2
		S12	55.4 ± 2.9

The change in composition of AMMCs affects their hardness [40]. In the case of Al-SiC, hardness increases with the increase in wt% of SiC as shown in Figure 8, whereas the reverse was observed in the case of Al-$ZrSiO_4$ (Figure 9). Moreover, for hybrid AMMCs, i.e., Al-SiC-$ZrSiO_4$, wt% of SiC enhanced the hardness, whereas $ZrSiO_4$ tried to pull it down as presented in Figure 10. Therefore, minimum levels of hardness of machined profiles were achieved at 40% of $ZrSiO_4$ in the case of both hybrid and binary AMMCs. All the results above showed that the hardness of machined samples is greatly influenced by the sintering temperature and the concentration of supplements. It is evident from the below plots that predicted and actual hardness correspond to one another in the case of Al-$ZrSiO_4$ binary composites and Al-SiC-$ZrSiO_4$ hybrid composites. In the case of Al-SiC, the trend of actual and predicted results is the same, but the composites did not correspond exactly to one another. ANOVA and regression equations were generated for the compliance of the experimental results. In the case of binary AMMCs of Al-$ZrSiO_4$, ANOVA showed that the sintering temperature and wt% produce significant values.

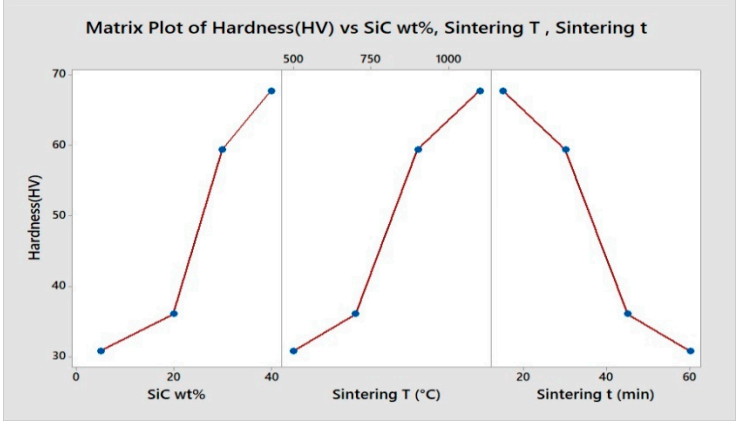

Figure 8. Main effect plot for machined Al-SiC.

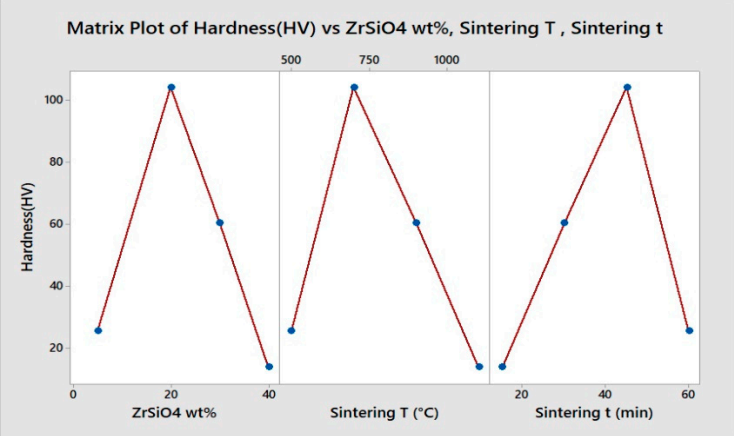

Figure 9. Main effect plot for machined Al-$ZrSiO_4$.

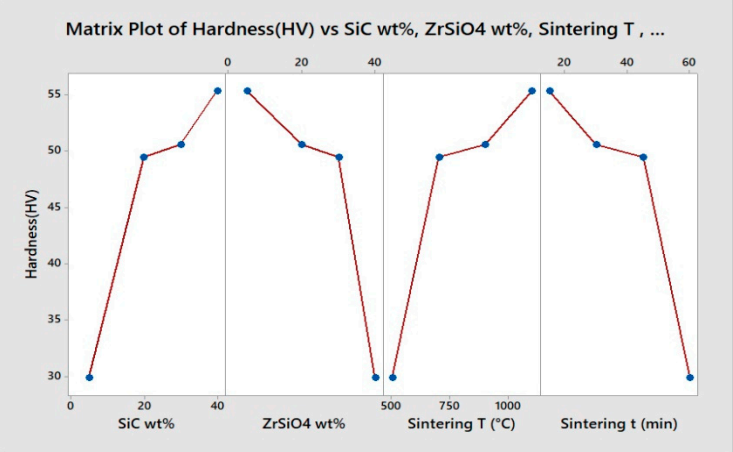

Figure 10. Main effect plot for Hybrid AMMCs.

3.4. Regression Analysis for Hardness of Machined Samples

The experimental values were then validated and tested against the predicted values by using regression analysis and ANOVA. Few observations had a substantial impact on the model prediction according to the study of the main effect plot, with some data having a stronger influence on the anticipated values than other. To pinpoint the reasons of these data, by improving the experimental design, we could increase the precision of the model predictions. In general, the plots are a useful tool for locating significant observations

and enhancing the prediction model's precision [30,41]. Equation (1) shows the relation between the hardness of machined samples of Al-SiC-$ZrSiO_4$ against input parameters, respectively.

$$\text{Hardness (HV)} = 634.92 + 24.835\ ZrSiO_4\ \text{wt\%} - 1.4673\ \text{Sintering T (°C)}. \quad (1)$$

The regression equation presented the same behavior as that which the experimental results showed. However, there was no significant factor ($p > 0.05$) found in the case of the hardness of machined AMMCs supplemented with SiC and the hybrid of SiC and $ZrSiO_4$. In the case of Al- $ZrSiO_4$, Equation (1) completely satisfied the statistical requirements observed in ANOVA, as sintering temperature and composition show significant values ($p < 0.05$).

However, the comparison graphs of predicted and experimental values for hardness at different levels of temperature and compositions showed a similar trend in the case of Al-SiC AMMCs, and they are exactly lying over one another in the case of Al-$ZrSiO_4$ and hybrid AMMCs as shown in Figure 11.

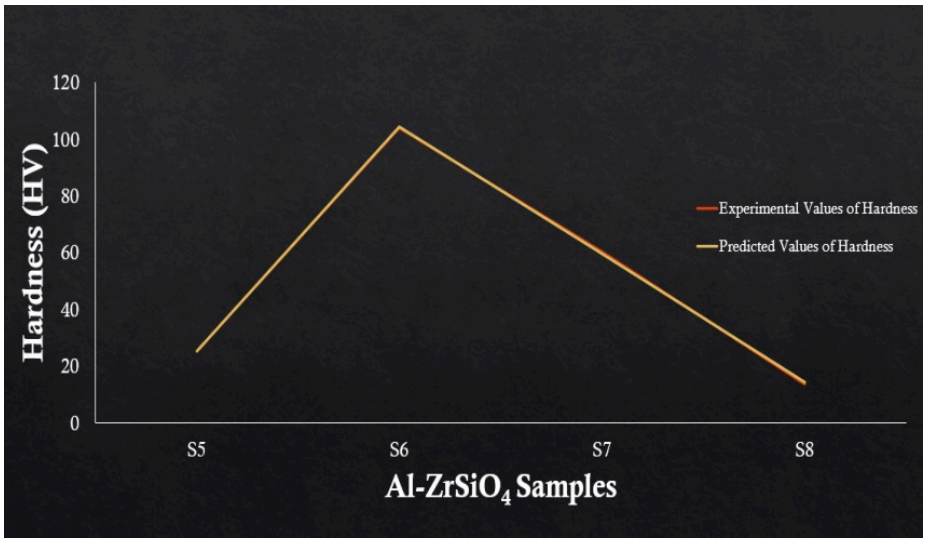

Figure 11. Comparison of experimental and predicted hardness values.

3.5. Recast Layer

The recast layer is fine-grained, hard, brittle, and different from its parent material structure. The formation of these layers is the result of process parameters of machining and work-piece compositions [42]. The major reason for the presence of a recast layer is the improper flushing of eroded material during pulse-off time and higher current and nature of supplements added into MMCs [43]. In the current study, recast layers were also observed, which increased the hardness of AMMCs. The white layer known as the recast layer appeared on the machined surface with cracks and micro voids, which can be seen via SEM (Figure 12).

Here, it is also important to note that SiC particles are hard in nature, which can distort the recast layer and result in cracks, voids, and phase transformations. This can cause drastic changes in the surface properties of the machined profile. The current study can be extended by investigating the surface properties of these AMMCs. Proper selection of wt% of reinforcements and peak current are the two most significant factors affecting the quality and thickness of the recast layer [44]. In the present study, WEDM parameters were kept constant on specific machining conditions, but by varying the machining conditions, significant results can be found which may contribute a lot to the available research regarding surface studies of AMMCs. In the future, this study can be extended for the optimization of machining parameters for such composites and cover the currently needed area to explore.

Parametric analysis for the change in thickness of the recast layer would also contribute to the new findings.

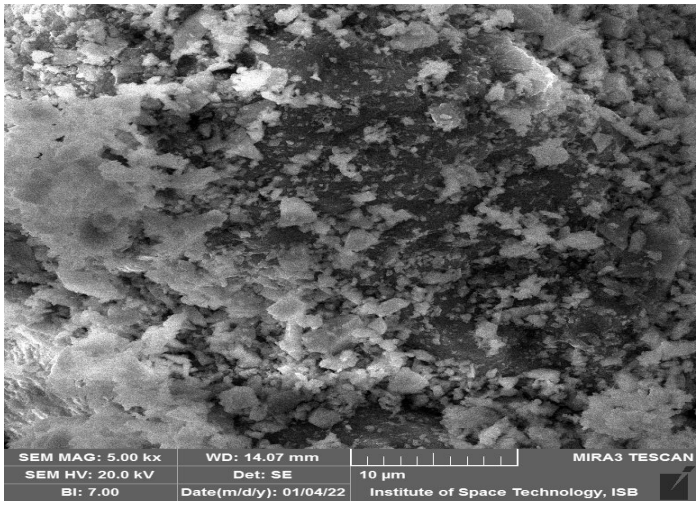

Figure 12. SEM image of Al-SiC sample showing white recast layer.

4. Conclusions

The conclusions drawn from the findings and discussions are listed below.

- EDS examination confirms the presence of SiC and $ZrSiO_4$ in the aluminum matrix machined samples, where the distribution of reinforcements is inferred from elemental analysis.
- The current investigation found that the machinability of each sample varies with wt%, the hardness of machined AMMCs is significantly affected by wt% of supplements, both individually and collectively. Since the strength of AMMCs must be improved [45], the high wt% of brittle SiC and $ZrSiO_4$ was added to the matrix alloy; optimal machining conditions are required. The machined profile becomes harder as the SiC weight percentage rises.
- The morphology of the AMMCs changes as a result of the addition of different reinforcements to the metal matrix.
- Particulate-rich and particulate-depleted zones are formed by the aggregation or clustering of the supplements of various shapes and sizes. This is a result of liquid phase sintering occurring at higher temperatures, specifically 1100 °C, which causes heterogeneous distribution and, ultimately, agglomeration and segregation [46].
- During sintering, supplements mix with molten matrix material at high temperatures in the liquid phase to create detrimental phases. Because SiC (3.21 g/cm^3) and $ZrSiO_4$ (4.56 g/cm^3) have different densities, aggregation occurs as the reinforcement particles slide on the molten metal. This can be prevented by using a two-stage addition of reinforcement particles [47], as opposed to the single-stage addition used here.
- As there is no significant relationship between sintering time and compaction pressure, sintering time for both machined and sintered samples does not significantly affect the hardness of either [48].
- The regression equations of HAMMC Al-SiC-$ZrSiO_4$ and machined Al-$ZrSiO_4$ satisfy the statistical criteria for ANOVA tables.
- From the microstructure, it can be shown that samples are sintered by liquid-state sintering rather than solid-state sintering as temperature and the proportion of reinforcements increase.
- Additionally, when the weight percentage of $ZrSiO_4$ raises, dendritic gaps and porosity are seen in the microstructure, resulting in a brittle structure. This is may be due to slow cooling.

Supplementary Materials: The following supporting information can be downloaded at: https://www.mdpi.com/article/10.3390/cryst13091347/s1.

Author Contributions: Conceptualization, M.R.B. and F.G.; methodology, T.Z.; software, U.G.; validation, S.B. and M.R.B.; formal analysis, F.G.; investigation, T.Z.; resources, U.G.; data curation, S.B.; writing—original draft preparation, M.R.B. and F.G.; writing—review and editing, U.G. and S.B; visualization, T.Z.; supervision, S.B.; funding acquisition, U.G. and M.R.B. All authors have read and agreed to the published version of the manuscript.

Funding: This work was supported by the National Research Foundation (NRF) of Korea through the Auspices of the Ministry of Science and ICT, Republic of Korea, under Grant NRF-2020R1G1A1012741.

Institutional Review Board Statement: Not applicable.

Informed Consent Statement: Not applicable.

Data Availability Statement: Data used to make the manuscript can be made available from the corresponding author(s) on reasonable request.

Conflicts of Interest: The authors declare no conflict of interest.

References

1. Kawahara, M.; Kato-Negishi, M. Link between Aluminum and the Pathogenesis of Alzheimer's Disease: The Integration of the Aluminum and Amyloid Cascade Hypotheses. *Int. J. Alzheimer's Dis.* **2011**, *2011*, e276393. [CrossRef]
2. Manish, S.; Dhakad, S.K.; Agarwal, P.; Pradhan, M.K. Review on Various Aluminum Based Metal Matrix Composite. *Int. J. Eng. Res.* **2018**, *6*, 2. [CrossRef]
3. Rajak, D.K.; Pagar, D.D.; Kumar, R.; Pruncu, C.I. Recent progress of reinforcement materials: A comprehensive overview of composite materials. *J. Mater. Res. Technol.* **2019**, *8*, 6354–6374. [CrossRef]
4. Kim, D.-Y.; Choi, H.-J. Recent Developments towards Commercialization of Metal Matrix Composites. *Materials* **2020**, *13*, 2828. [CrossRef]
5. Dubey, A.K.; Yadava, V. Laser Beam Machining—A Review. *Int. J. Mach. Tools Manuf.* **2008**, *48*, 609–628.
6. Yigezu, B.S.; Jha, P.K.; Mahapatra, M.M. The Key Attributes of Synthesizing Ceramic Particulate Reinforced Al-Based Matrix Composites through Stir Casting Process: A Review. *Mater. Manuf. Process.* **2013**, *28*, 969–979.
7. Pal, M.K.; Vikram, A.; Bajaj, V. Enhanced microstructure and mechanical properties of sic particle reinforced Aluminium alloy composite materials. *Acta Met. Slovaca* **2019**, *25*, 253–258. [CrossRef]
8. Ashkani, O.; Tavighi, M.R.; Karamimoghadam, M.; Moradi, M.; Bodaghi, M.; Rezayat, M. Influence of Aluminum and Copper on Mechanical Properties of Biocompatible Ti-Mo Alloys: A Simulation-Based Investigation. *Micromachines* **2023**, *14*, 1081. [CrossRef]
9. Gillani, F.; Khan, M.Z.; Shah, O.R. Sensitivity Analysis of Reinforced Aluminum Based Metal Matrix Composites. *Materials* **2022**, *15*, 4225. [CrossRef]
10. Meena, K.L.; Manna, A.; Banwait, S.S. An Analysis of Mechanical Properties of the Developed Al/SiC-MMC's. *Am. J. Mech. Eng.* **2013**, *1*, 14–19.
11. Das, D.; Mishra, P.C.; Chaubey, A.K.; Samal, C. Characterization of the developed aluminium matrix composites-an experimental analysis. *Mater. Today Proc.* **2018**, *5*, 3243–3249. [CrossRef]
12. Rizwee, M.; Minz, S.S.; Orooj, M.; Hassnain, M.Z.; Khan, M.J. Electric Discharge Machining Method for Various Metal Matrix Composite Materials. *Int. J. Innov. Technol. Explor. Eng. (IJTEE)* **2019**, *8*, 1796–1807. [CrossRef]
13. Choudhary, S.K.; Jadoun, R.S. Current Advanced Research Development of Electric Discharge Machining (EDM): A Review. *Int. J. Res. Advent Technol.* **2014**, *2*, 273–297.
14. Li, J.; Chen, W.; Zhu, Y. Study on Generating Machining Performance of Two-Dimensional Ultrasonic Vibration-Composited Electrolysis/Electro-Discharge Technology for MMCs. *Materials* **2022**, *15*, 617. [CrossRef]
15. Gillani, F.; Zahid, T.; Bibi, S.; Khan, R.S.U.; Bhutta, M.R.; Ghafoor, U. Parametric Optimization for Quality of Electric Discharge Machined Profile by Using Multi-Shape Electrode. *Materials* **2022**, *15*, 2205. [CrossRef] [PubMed]
16. Abu Qudeiri, J.E.; Saleh, A.; Ziout, A.; Mourad, A.-H.I.; Abidi, M.H.; Elkaseer, A. Advanced Electric Discharge Machining of Stainless Steels: Assessment of the State of the Art, Gaps and Future Prospect. *Materials* **2019**, *12*, 907. [CrossRef]
17. Rajkumar, K.; Poovazhagan, L.; Selvakumar, G.; Muthukumar, B. Wire Electrical Discharge Machining Integrity Studies on the Aluminium Nanocomposite. In *Advances in Manufacturing Processes*; Springer: Berlin/Heidelberg, Germany, 2019; pp. 543–554. [CrossRef]
18. Rezayat, M.; Karamimoghadam, M.; Ashkani, O.; Bodaghi, M. Characterization and Optimization of Cu-Al_2O_3 Nanocomposites Synthesized via High Energy Planetary Milling: A Morphological and Structural Study. *J. Compos. Sci.* **2023**, *7*, 300. [CrossRef]
19. Hashim, J.; Looney, L.; Hashmi, M.S.J. Particle distribution in cast metal matrix composites—Part I. *J. Mater. Process. Technol.* **2002**, *123*, 251–257. [CrossRef]
20. Levashov, E.; Kurbatkina, V.; Alexandr, Z. Improved Mechanical and Tribological Properties of Metal-Matrix Composites Dispersion-Strengthened by Nanoparticles. *Materials* **2010**, *3*, 97–109. [CrossRef]

21. Dhupal, D.; Naik, S.; Das, S.R. Modelling and Optimization of Al–SiC MMC through EDM Process Using Copper and Brass Electrodes. *Mater. Today Proc.* **2018**, *5*, 11295–11303. [CrossRef]
22. Gavisiddesha, P.; Thotappa, C.; Algur, V.; Suresh Reddy, B. Optimization of Wire Cut Electric Discharge Machining Characteristics of Hybrid Aluminium Composites (Al6061/Gr/SiCp) Using Taguchi Method. In *Sustainable Machining Strategies for Better Performance*; Springer: Berlin/Heidelberg, Germany, 2022; pp. 49–60.
23. Feldshtein, E.E.; Dyachkova, L.N.; Patalas-Maliszewska, J. On Investigating the Microstructural, Mechanical, and Tribological Properties of Hybrid FeGr1/SiC/Gr Metal Matrix Composites. *Materials* **2021**, *14*, 174. [CrossRef]
24. Karabulut, Ş.; Karakoç, H.; Çitak, R. Effect of the B4C Reinforcement Ratio on Surface Roughness of A16061 Based Metal Matrix Composite in Wire-EDM Machining. In Proceedings of the 2017 8th International Conference on Mechanical and Aerospace Engineering (ICMAE), Prague, Czech Republic, 22–25 July 2017; IEEE: Piscataway, NJ, USA, 2017; pp. 812–815.
25. Bains, P.S.; Sidhu, S.S.; Payal, H.S. Fabrication and Machining of Metal Matrix Composites: A Review. *Mater. Manuf. Process.* **2016**, *31*, 553–573. [CrossRef]
26. Abbas, N.M.; Solomon, D.G.; Bahari, M.F. A review on current research trends in electrical discharge machining (EDM). *Int. J. Mach. Tools Manuf.* **2007**, *47*, 1214–1228. [CrossRef]
27. Ramasawmy, H.; Blunt, L. Effect of EDM process parameters on 3D surface topography. *J. Mater. Process. Technol.* **2004**, *148*, 155–164. [CrossRef]
28. Kannan, V.S.; Lenin, K.; Srinivasan, D.; Kumar, D.R. Investigation on Laser Square Hole Drilling of AA7475/SiC/$ZrSiO_4$ Composites. *Silicon* **2022**, *14*, 4557–4574. [CrossRef]
29. Krishna, S.M.; Shridhar, T.N.; Krishnamurthy, L. Research Significance, Applications and Fabrication of Hybrid Metal Matrix Composites. *Int. J. Innov. Sci. Eng. Technol.* **2015**, *2*, 227–237.
30. Rezayat, M.; Karamimoghadam, M.; Yazdi, M.S.; Moradi, M.; Bodaghi, M. Statistical analysis of experimental factors for synthesis of copper oxide and tin oxide for antibacterial applications. *Int. J. Adv. Manuf. Technol.* **2023**, *127*, 3017–3030. [CrossRef]
31. Gururaja, S.; Ramulu, M.; Pedersen, W. Machining of MMCS: A Review. *Mach. Sci. Technol.* **2013**, *17*, 41–73. [CrossRef]
32. Pramanik, A.; Basak, A.; Prakash, C. Understanding the wire electrical discharge machining of Ti6Al4V alloy. *Heliyon* **2019**, *5*, e01473. [CrossRef]
33. Pramanik, A.; Basak, A.K.; Dixit, A.R.; Chattopadhyaya, S. Processing of duplex stainless steel by WEDM. *Mater. Manuf. Process.* **2018**, *33*, 1559–1567. [CrossRef]
34. Mussada, E.K.; Hua, C.C.; Rao, A.K.P. Surface hardenability studies of the die steel machined by WEDM. *Mater. Manuf. Process.* **2018**, *33*, 1745–1750. [CrossRef]
35. Kar, S.; Patowari, P.K. Electrode wear phenomenon and its compensation in micro electrical discharge milling: A review. *Mater. Manuf. Process.* **2018**, *33*, 1491–1517. [CrossRef]
36. Gostimirovic, M.; Kovac, P.; Sekulic, M.; Skoric, B. Influence of discharge energy on machining characteristics in EDM. *J. Mech. Sci. Technol.* **2012**, *26*, 173–179. [CrossRef]
37. Arikatla, S.P.; Mannan, K.T.; Krishnaiah, A. Parametric Optimization in Wire Electrical Discharge Machining of Titanium Alloy Using Response Surface Methodology. *Mater. Today Proc.* **2017**, *4*, 1434–1441. [CrossRef]
38. Muthuramalingam, T.; Mohan, B. A review on influence of electrical process parameters in EDM process. *Arch. Civ. Mech. Eng.* **2015**, *15*, 87–94. [CrossRef]
39. El-Kady, O.; Fathy, A. Effect of SiC particle size on the physical and mechanical properties of extruded Al matrix nanocomposites. *Mater. Des.* **2014**, *54*, 348–353. [CrossRef]
40. Srivastava, A.K.; Dixit, A.R.; Tiwari, S. A review on the intensification of metal matrix composites and its nonconventional machining. *Sci. Eng. Compos. Mater.* **2018**, *25*, 213–228. [CrossRef]
41. Moradi, M.; Karamimoghadam, M.; Meiabadi, S.; Casalino, G.; Ghaleeh, M.; Baby, B.; Ganapathi, H.; Jose, J.; Abdulla, M.S.; Tallon, P.; et al. Mathematical Modelling of Fused Deposition Modeling (FDM) 3D Printing of Poly Vinyl Alcohol Parts through Statistical Design of Experiments Approach. *Mathematics* **2023**, *11*, 3022. [CrossRef]
42. Paswan, K.; Chattopadhyaya, S.; Pramanik, A. A Review Paper on Machining of Metal Matrix Composite and Optimizing Methods used in Electrical Discharge Machining. *Mater. Today Proc.* **2018**, *5*, 24428–24438. [CrossRef]
43. Vignesh, S.; Mohan, B.; Muthuramalingam, T.; Karthikeyan, S. Evaluation of Recast Layer Thickness of Electrical Discharge Machined AISI 202 Stainless Steel with Various Pulse Generators. In *Proceedings of the Applied Mechanics and Materials*; Trans Tech Publications: Bach, Switzerland, 2015; Volume 766, pp. 518–522.
44. Singh Sidhu, S.; Singh Bains, P. Study of the Recast Layer of Particulate Reinforced Metal Matrix Composites machined by EDM. *Mater. Today Proc.* **2017**, *4*, 3243–3251. [CrossRef]
45. Kaviyarasan, K.; Kumar, J.P.; Anandh, S.K.; Sivavishnu, M.; Gokul, S. Comparison of mechanical properties of Al6063 alloy with ceramic particles. *Mater. Today Proc.* **2020**, *22*, 3067–3074. [CrossRef]
46. Haanappel, S.; Thije, R.T.; Sachs, U.; Rietman, B.; Akkerman, R. Formability analyses of uni-directional and textile reinforced thermoplastics. *Compos. Part A: Appl. Sci. Manuf.* **2014**, *56*, 80–92. [CrossRef]

47. Olakanmi, E.O.T.; Cochrane, R.F.; Dalgarno, K.W. A review on selective laser sintering/melting (SLS/SLM) of aluminium alloy powders: Processing, microstructure, and properties. *Prog. Mater. Sci.* **2015**, *74*, 401–477. [CrossRef]
48. Kumar, G.V.; Rao, C.P.; Selvaraj, N. Mechanical and Tribological Behavior of Particulate Reinforced Aluminum Metal Matrix Composites—A review. *J. Miner. Mater. Charact. Eng.* **2011**, *10*, 59–91. [CrossRef]